Journal of Engineering Physics and Thermophysics, Vol. 70, No. 4, 1997

EXPERIMENTAL STUDY OF A HETEROGENEOUS PLASMA FLOW IN A REACTOR WITH A MULTIJET MIXING CHAMBER

V. D. Shimanovich, A. L. Mossé,
L. E. Krat'ko, N. I. Chubrik,
E. A. Ershov-Pavlov, E. M. Ermolaeva, and
A. N. Knak

UDC 533.9

Results of opticospectroscopic measurements of a plasma flow containing particles of different materials (Al_2O_3, SiO_2, kaolin, phosphorite, and chamotte sand) at the outlet of the mixing chamber of a plasma reactor are reported.

Introduction. Multiarc plasma reactors are widely employed for investigations and implementation of various technological processes. The main unit in such reactors is a cylindrical or conic mixing chamber into which several plasma generators symmetrically installed on the lateral generatrix of the chamber operate. The efficiency of the process depends in many respects on the conditions of plasma flow formation in the mixing chamber and input of particles of a raw material [1]. To obtain quantitative characteristics of a plasma flow and the dispersed particles moving in it, it is necessary to know the distributions of local velocity and flow temperature with respect to the cross-section and channel length of the reactor, particle trajectories, their temperatures and velocities. Theoretical and experimental studies of a heterogeneous plasma flow are required for obtaining dimensionless relations describing heat transfer processes in a plasma reactor and for the development of adequate mathematical models for design of plasma generators and optimization of the technological regimes in them. A heterogeneous plasma jet is characterized by complicated phase and element compositions. Due to plasma action there occur heating, fusion of particles of the solid phase, as well as material evaporation from the surface of solid particles. In its turn, a material introduced into a plasma in powder form changes the composition and properties of the plasma. Below we report results of opticospectroscopic measurements of the parameters of a plasma flow formed in the three-jet conic mixing chamber of a plasma reactor containing particles of different materials. Results of diagnostics of a heterogeneous plasma jet are provided: the space-time characteristics of the plasma flow are described, the temperatures and velocities of the plasma jets and powder particles are determined under different conditions, the component composition of the plasma is evaluated, a comparative analysis of the plasma radiation and particles of the solid phase is made.

1. Experimental setup and method for measuring the parameters of heterogeneous plasma jets. The experimental setup consisted of three PDS-3 plasma generators, whose anodes had a 17 mm smooth channel, a conic mixing chamber with a taper angle of 60°, ten water-cooled sections of the reactor channel, a raw material feeder, and systems of electric power, gas and water supply. The plasma reactor, having a chamber diameter of 100 mm and a length of each section of 19 mm, was positioned horizontally in space. For spectral measurements the reactor channel had special slits of 4-6 mm. As a dispersed material, use was made of powders of alumina and silicon dioxide as well as of phosphorite, kaolin, and chamotte sand. Particle diameters were 120 μm for Al_2O_3, 100–130 μm for phosphorite, 200 μm for SiO_2, 50 μm for kaolin, and 200–300 μm for chamotte sand.

Opticospectroscopic measurements included high-speed photography of plasma flows with a dispersed phase and recording of the spectra of their radiation. Images of the plasma jets were simultaneously projected by two

---

Institute of Molecular and Atomic Physics of the Academy of Sciences of Belarus; Academic Scientific Complex "A. V. Luikov Heat and Mass Transfer Institute of the Academy of Sciences of Belarus," Minsk, Belarus.
Translated from Inzhenerno-Fizicheskii Zhurnal, Vol. 70, No. 4, pp. 560-568, July-August, 1997. Original article submitted March 24, 1997.

1062-0125/97/7004-0559$18.00 ©1997 Plenum Publishing Corporation

different optical systems onto motion-picture film and the inlet slit of the spectrograph. Simultaneous radiation recording by both systems ensured correspondence of optical and spectroscopic measurement data. The devices and the scheme of opticospectroscopic measurements are described in [2].

1.1. Evaluation of the Component Composition of Plasma. Preliminary investigation have shown that the composition of a plasma jet differs considerably from the plasma composition determined by a plasma-forming gas (air). The spectrum of plasma radiation in the absence of a solid dispersed phase shows, in addition to spectral lines corresponding to the components of a "pure" air plasma, lines attributed to the presence of erosion products (copper) of the nozzle-anode as well as the lines of calcium atoms and ions present in the working gas as natural impurities. With the introduction of a solid dispersed phase some spectral lines appear in the radiation spectrum of the "dust-laden" plasma which pertain to evaporation products of the powder particles and additives constituting it. It should be noted that easily ionizable admixtures substantially change the plasma parameters and in many respects determine its properties. The degree of this influence depends on the operation parameters of the installation and the range of plasma parameters.

Thus, for each particular set of operation conditions it is necessary to know the component composition of the plasma. For this, we employed measurement results of the relative distribution of the intensity of different components (spectral lines) in the radiation spectrum of the plasma jet as well as calculation data on air plasma composition with an admixture of the most influencing elements. Measuring the relative intensity of spectral lines of different components in the plasma radiation spectrum, we can determine the relative concentration of emitting particles, i.e., the relative component composition of the plasma in its limited temperature interval.

1.2. Measurement of Electron Concentration and Temperatures of Plasma and Particles. The temperature of the investigated plasma is rather low. This circumstance does not allow use of the radiation of plasma-forming gas components that possess rather high excitation potentials for measurement of its parameters. Therefore for plasma diagnostics we used, as the reference data, the emissive power (intensity) of the atomic lines of copper present in the plasma as a result of anode erosion. It was assumed that the products of anode erosion penetrated into the plasma and were uniformly intermixed in the entire plasma flow. The plasma temperature was measured by the relative intensity of the lines [3] of copper atoms of the same ionization degree. These measurements did not require additional restrictions on the conditions of the plasma ionization state or knowledge of the electron concentration in the plasma. The electron concentration (n_e) was calculated at a known temperature by the relative emissive power (intensity) of the Ca atom and ion lines.

Spectroscopic diagnostics was carried out under the assumption that the plasma was in a state close to the LTR, the difference between the temperatures of electrons and atoms was small, and the plasma jet was transparent in the spectral ranges chosen for measurements [4]. In passing from the measured spectral intensity of a plasma flow to the local parameters of the plasma we used the localization method [5]. The latter possesses a number of advantages as compared to the widely adopted Abel inversion [6].

The temperature of powder particles in the plasma was measured by the relative intensity of the continuum caused by the simultaneous irradiation of the particles and the plasma at 650 and 680 nm.

1.3. Calculation of the Plasma Composition. The electron concentration obtained was used to refine the component composition of the plasma. Based on the relative intensity of lines of different components, the impurity elements were determined which exerted a pronounced influence on the plasma properties. For various types of dispersed phase the elements were different, however, as a rule, it was possible to determine the dominating one. Next, for the prescribed temperature we calculated the composition of the plasma-forming gas with the chosen element as the impurity. To simplify the calculation, we choose nitrogen instead of air (as the plasma-forming gas). The composition of the nitrogen plasma insiginificantly differs from that of the air plasma [7]. Molecular components were not taken into account in the calculation. The impurity content was determined from the measured electron concentrations.

2. Results of diagnostics of heterogeneous plasma jet. *2.1. Space-Time Characteristics of Plasma Flow.* As high-speed camera investigations of the space-time characteristics of plasma flows without a dispersed phase have shown [4], the generated plasma represents a collection of inhomogeneous unsteady-state jets with pulsation

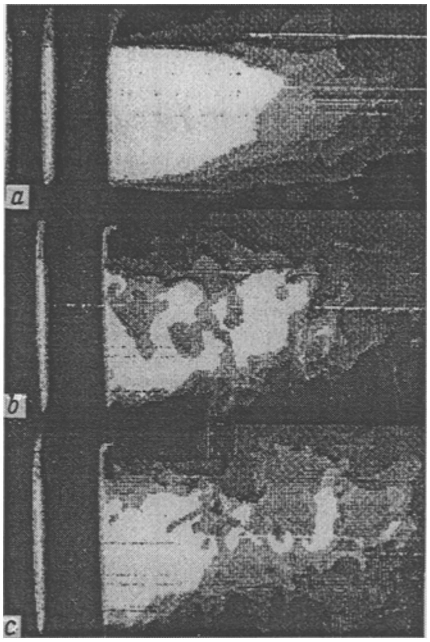

Fig. 1. Photo of SiO_2-particle-containing plasma jet at outlet of reactor channel obtained by a video camera with exposure of 20 msec (a) and 250 μsec (b, c) and processed on a personal computer (c).

frequencies predominantly in the range of 5–10 kHz. In order to trace the behavior of a plasma jet with a dispersed phase under different conditions, similar investigations were carried out using video and high-speed cameras.

The plasma flare at the reactor outlet (after the 10th measuring section, $l = 194$ mm from the mixing chamber outlet) was filmed by a "Panasonic" camera. To obtain resolution of the space-time characteristics, we used a maximum exposure of 0.25 msec. Then the data obtained were input into a computer and represented by four levels of brightness for better representation of the spatial structure. Photos showing the turbulent character of the flare are given in Fig. 1. The photo taken with an exposure of 20 msec (Fig. 1a) depicts a jet without spatial details, i.e., as it was observed with the unaided eye. SiO_2 particles present in the plasma flow are not seen in the figure, because of their relatively small size (the filming was done at a distance of 3 m). The photos taken with a time resolution of 250 μsec (Fig. 1b, c) indicate that the jet at the outlet of the sectionalized reactor channel consists of plasmoids randomly distributed in the flow. To make spectral measurements with a time resolution sufficient for resolution of the instantaneous spatial structure of a jet, it is necessary to have special devices such as, for instance, those used in [8].

Results of the independent high-speed filming confirm the characteristic time of existence of a plasmoid at a given point in space of ~0.25 msec, i.e., a further increase in time resolution will provide no additional details in the spatial structure of the flare. Spectroscopic temperature measurements made with respect to time-averaged spectra for times equal to tenths and units of seconds have shown that the radiation of the plasma jet attenuates and one can observe tracks due to emission of heated particles of the solid phase at distances of $l \sim 75-100$ mm.

Based on the high-speed photoregistrograms obtained, evaluation was made of velocities of the plasma jets and powder particles in different conditions. Data on the velocities are given in Table 1. Separate plasma jets and particles in the flow are characterized by some variations in velocities. The values of $W_{\max}$ for plasma jets pertain to mean velocities at distances of $l \sim 5-25$ mm, while those of $W_{\min}$ – at distances of $l \sim 50-75$ mm from the mixing chamber outlet. Powder particles are accelerated in the plasma flow and over the section from $l \sim 50-75$ mm up to $l \sim 150$ mm they fly with a constant speed. This section of the jet contains the minimum ($W_{\min}$) and maximum ($W_{\max}$) velocities of the particle flux. At distances of $l \sim 150$ mm, the intensity of particle emission decreases, which does not allow velocity measurements to be made by this method.

As seen from the table, the velocities of plasma jets markedly increase with an increase in the gas flow rate from 2.5 to 4 g/sec. Their increase with electrical power is insignificant. At the same time an increase in the powder

TABLE 1. Measurement Results for Plasma Flow and Al_2O_3-Particle Velocities for Different Operation Conditions of the Installation

Operation parameters, I, A/ U, V/ G_g, g/sec/ G_p, g/sec	W, m/sec, min-max	
	plasma	particles
165/210/2.5/1.5	32–80	–
205/230/4.0/1.5	45–125	46–77
140/240/4.0/1.5	31–111	60–82
165/210/2.5/1.7	20–35	32–53
165/210/2.5/2.1	16–23	35–46

flow rate from 1.5 to 2.1 g/sec causes a slight decrease in the velocity of jets. The data on particle velocities show the same dependences on operation conditions as the plasma jets though they are less pronounced.

2.2. Qualitative Analysis of Spectra. Radiation spectra of a "pure" plasma jet and a plasma jet containing particles of different powder materials considerably differ. In the absence of a dispersed phase, the spectrum consists mainly of the radiation lines CuI, CaI, CaII, NaI and traces of N_2, CaO, and CuO molecules. In the radiation spectra of a plasma jet containing Al_2O_3 powder particles we observe intense lines AlI, an increase in the intensity of lines NaI, and appearance of the highest-intensity bands of an AlO molecule extending from 400 to 550 nm. Moreover, in the spectra the spectral lines belonging to impurities of such elements as Ba, Li, K, Ga, Sr, Fe, Ti, Mn have been detected.

An analysis of the radiation spectra of a plasma jet with phosphates and SiO_2 particles as well as with kaolin and chamotte sand shows that the spectra consist mainly of spectral lines and molecular bands of the same elements as in the case of Al_2O_3 particles. The difference lies in the relative content of these elements in the jet. For each of the investigated powders only one or two elements exert a determining influence on the radiation spectrum. Those are Al, Ca, and Na. With respect to the content of these elements the investigated powders can be arbitrarily separated into aluminum-sodium- and calcium-containing groups. The first group includes Al_2O_3, kaolin and chamotte sand, while SiO_2 and phosphates are assigned to the second group. Radiation spectra of a plasma jet with particles belonging to the same group are similar. A jet containing phosphates and SiO_2 is distinguished with the active formation of CaO and CaF molecules, whose bands are observed in the range 550–650 nm.

The distribution of different elements over the cross-section of the plasma flow is rather uniform. Such an intensity distribution is characteristic for axisymmetrical inhomogeneous sources.

2.3. Component Composition of Plasma. A plasma jet of "pure" air plasma contains erosion products of the anode material, i.e., copper. As estimates have shown [4], for the operation conditions of the present electric-arc installation the copper concentration in the jet is 0.001%. We used this value as a reference value for estimation of the relative content of other elements upon introducing a dispersed phase into the jet. Based on the calculated coefficients and the measured radiation intensities of the lines it is shown that in the case of a jet without powder the concentration of impurities of calcium and sodium is $\sim 10^{-6}\%$. On introducing Al_2O_3 particles into the jet the amount of calcium does not change, but the concentration of sodium increases up to 0.001%, and that of aluminum, up to $10^{-4}-10^{-5}\%$, while the concentration of the remaining umpurities is less than $10^{-5}\%$. The relative concentration of those for a jet with kaolin and chamotte sand corresponds approximately to that described above. In a jet with SiO_2 powder the concentration of impurities is not very high: the amount of Na and Ca increases up to $10^{-5}\%$ and that of aluminum up to $10^{-6}\%$. In the case of a jet with phosphates the main element in the plasma is Ca, and its amount is approximately 10%.

The concentration of impurities in the jet slightly changes depending on the distance from the mixing chamber outlet. Figure 2 shows radiation intensities of the spectral lines of Na, Al and the edge of the AlO band for a jet with Al_2O_3 particles which reflect the relative concentration of these elements with variation of the distance

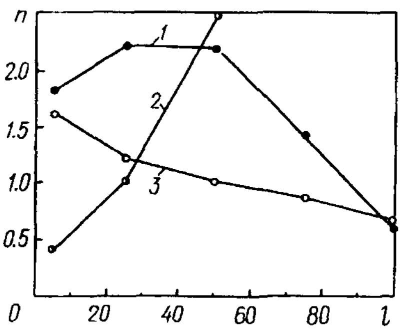

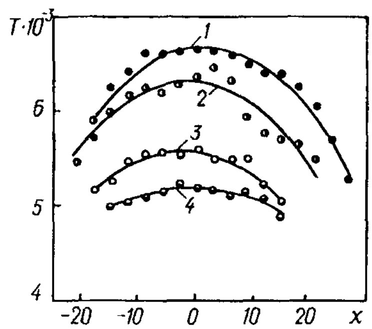

Fig. 2. Distribution of relative concentration of different components in plasma along Al_2O_3-containing jet: 1) AlO, 2) Na, 3) Al. *n*, rel. units.

Fig. 3. Cross-sectional plasma-temperature distribution in plasma jet without powder at different distances from mixing chamber outlet: 1) 5 mm, 2) 25 mm, 3) 50 mm, 4) 75 mm.

from the mixing chamber outlet up to 100 mm. As is seen, the most intense evaporation of the impurities from powder particles proceeds in the part of the jet from the section up to 50 mm. Thus, the amount of Na in this zone increases by approximately a factor of 5. There, the most enhanced formation of AlO molecules occurs. Some decrease in the aluminum concentration is likely to be associated with the fact that some atoms participate in the formation of AlO molecules.

The calculation of plasma composition using experimental data on the content of impurities in the plasma jet with the presence of different powder materials in it allowed us to obtain dependences of the electron concentration on the plasma temperature. In the range $T = 4000-6000$ K the electron concentration n_e of a phosphate-containing plasma jet increased from $2 \cdot 10^5$ to $5 \cdot 10^{16}$ cm^{-3}, which exceeded n_e for a plasma of the aluminum-sodium group by several orders of magnitude. For the latter the electron concentration at a temperature of about 4000 K was $8 \cdot 10^{12}$ cm^{-3}, which exceeded that for a plasma with erosion products by an order of magnitude, and for a "pure" nitrogen plasma, by two orders. At $T > 6000$ K differences, with the exception of the plasma with phosphates, were insignificant.

2.4. Results of Plasma Temperature Measurements. Jet cross-section temperature distributions of a plasma without a dispersed phase at different distances from the mixing chamber, outlet measured by the relative intensity of spectral CuI lines are shown in Fig. 3. The data are obtained for the main operation conditions of the installation (the mean values of the parameters for each of the plasma generators are: $I = 165$ A, $U = 210$ V, $G_g = 2.5$ g/sec). As seen, the distributions are of a parabolic form and sufficiently symmetrical relative to the center of the mixing chamber. The maximum temperature at the outlet of the mixing chamber in the central zones of the jet attains ~6600 K and decreases to 5000 K at a distance of $l = 75$ mm. The diameter of the high-temperature zone of the jet is ~50–60 mm.

When powder particles are introduced into a plasma jet, the choice of diagnostic components becomes problematic. In the majority of cases the main diagnostic lines, i.e., CuI, are inapplicable for measurements. For the aluminum-sodium group those lines are overlapped with the bands of an AlO molecule; for phosphate-containing jets, their intensity is insufficient for measurements, because of a considerable decrease in temperature. Only for a plasma with SiO_2 particles can measurements be made using the lines CuI since the amount of impurities penetrating into the jet for this powder is minimum as compared to others. Figure 4 shows the cross-sectional temperature destribution at distance $l = 22$ mm from the mixing chamber outlet (after the first measuring section) for a SiO_2-containing plasma jet for the main operating regime with a powder flow rate of 1.5 g/sec. Since in this case the amount of easily ionized impurities is small, the plasma temperature decreases insignificantly (by ~200 K) as compared to a "pure" plasma jet.

In diagnostics, for a phosphate-containing plasma jet we used the relative intensity of the 657.3 and 646.3 nm CaI lines. Measurement results for two distances from the outlet of the mixing chamber are shown in Fig. 5. A high Ca concentration in the jet (with an ionization potential of 6.1 eV) causes a considerable decrease in

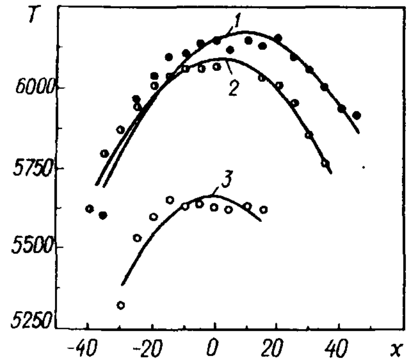

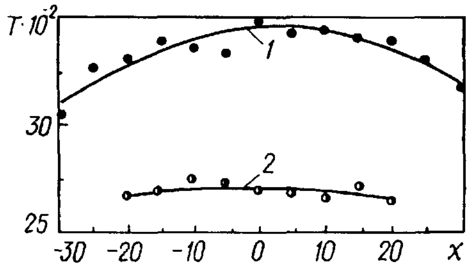

Fig. 4. Cross-sectional plasma temperature distribution in plasma jet with different powders: 1, 3) SiO_2 at distances of 22 and 108 mm, respectively; 2) kaolin at a distance of 22 mm.

Fig. 5. Cross-sectional plasma temperature distribution in plasma jet with phosphorite powder at different distances from chamber outlet: 1, 2) at distances of 22 and 108 mm, respectively, from mixing chamber outlet.

temperature to 4000 K (after the first measuring section, $l = 22$ mm), while at distance $l = 108$ mm (after the fifth section) the temperature decreases to 3200 K. The distributions are gently sloping and at distance $l = 10.8$ mm the jet becomes practically homogeneous.

For a plasma jet of the sodium-aluminum group plasma temperatures were measured by the relative intensity of the lines CaI and CaII (422.7 nm and 393.4 nm, respectively). Figure 6 shows cross-sectional temperature distributions of a plasma jet with Al_2O_3 particles at the outlet of the mixing chamber for powder flow rates of 1.7 g/sec (1) and 2.1 g/sec (2). As is seen, such an increase in the powder flow rate causes only an insiginifant decrease in the plasma temperature.

2.5. Comparative Analysis of Radiation of Plasma and Solid Particles. The radiation spectrum of the solid phase, unlike that of the gas phase and the plasma, consists only of a continuum. To measure the particle temperature of the solid phase by methods of optical spectrometry (pyrometry), it is necessary to separate the continuous radiation of particles from the total radiation of a heterogeneous jet. In the general case the radiation portion of powder particles in the total continuum of a heterogeneous plasma jet depends on the particle concentration in the jet, their sizes and temperature, as well as on the electron concentration and plasma temperature.

For comparative evaluation of the radiation intensity of plasma and particles in the solid phase we will choose standard operation conditions of the installation with the introduction of Al_2O_3 powder with a mean size of spherical particles of 75 μm. A powder flow rate is 1.5 g/sec, and their velocity in the plasma jet is 50 m/sec. Particles escape from a chamber with an outlet section of 100 mm and form a corresponding flow, which, for simplicity, will be assumed to be nondiverging (i.e., the particle concentration in the jet will be overestimated). Under such conditions with allowance for the Al_2O_3 density, the Al_2O_3 particle concentration in the plasma jet n_p is no more than 5 particles/cm^3. Calculation results for the emissivity of plasma with Al_2O_3 powder and Al_2O_3 particles are represented in Fig. 7. For comparison, the same figure shows the emissivity of a plasma whose composition corresponds to a phosphate powder-containing plasma jet (curves 4, 5). The size and the concentration of phosphate particles in the plasma jet are the same as for Al_2O_3 particles. The emissivity of the phosphate particles can differ only insignificantly from that of Al_2O_3 particles. Therefore, the calculation data for the radiation of the solid phase are applicable for both types of particles. As judged from the figure, the intensity of continuous radiation of the plasma depends considerably on its composition. A comparison of the given data shows that the radiation of particles at temperatures exceeding 2000 K prevails over that of a "pure" plasma as well as of an Al_2O_3 powder-containing plasma "contaminated" with 0.001% Na. When easily ionizable elements constituting the powder arrive in the plasma, the intensity of its radiation becomes comparable to or even exceeds that of particles, which hinders considerably measurements and increases their error. From the data obtained it follows that introduction of the

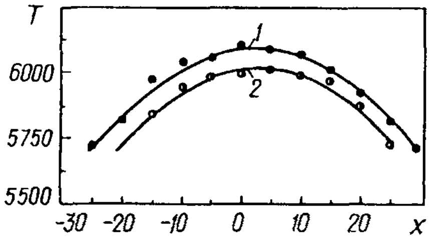

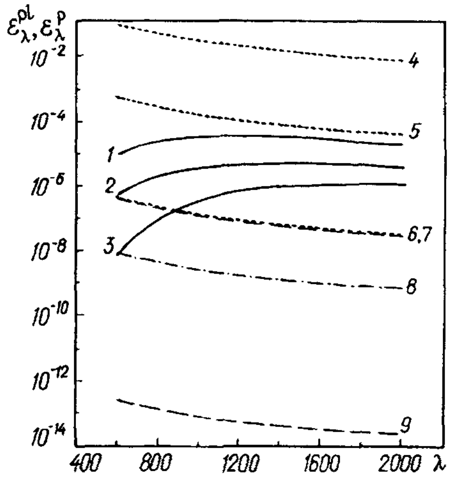

Fig. 6. Cross-sectional plasma temperature distribution in plasma jet with Al_2O_3 particles at outlet of mixing chamber for different powder flow rates: 1) 1.7 g/sec, 2) 2.1 g/sec.

Fig. 7. Total spectral emissivity of unit plasma volume ε_λ^{pl} and of Al_2O_3 particles in unit volume of plasma jet, ε_λ^{p} as a function of wavelength: 1, 2, 3) ε_λ^{p} – for particles at temperatures of 2500, 2000, and 1500 K, respectively; 4, 5) ε_λ^{pl} – of nitrogen plasma with 10% Ca at temperatures of 6000 and 4000 K, respectively; 6, 8) ε_λ^{pl} – of nitrogen plasma with 0.001% Na at temperatures of 6000 and 4000 K, respectively; 7, 9) ε_λ^{pl} – of nitrogen plasma at temperatures of 6000 and 4000 K, respectively.

phosphate powder into the plasma jet is accompanied by the ingress of a large amount of the easily ionizable impurity (up to 10% of Ca) into the plasma. As a consequence, the continuous plasma radiation, which even at a comparatively low temperature (T = 4000 K) considerably exceeds thermal radiation of powder particles practically in the entire investigated spectral region, abruptly enhances. In such conditions it is practically impossible to measure the temperature of a particle surface by the traditional methods of optical pyrometry.

With introduction of Al_2O_3 particles into the plasma jet, the concentration of the easily ionizable admixture becomes considerably lower (at a level of 0.001% Na). This allows separation of particle radiation against the background of continuous plasma radiation at least in the region of low (less than 4000 K) temperatures. With an increase in the temperature, the error of optical pyrometric temperature measurements drastically increases. Therefore the particle temperature measured at a distance of more than 50 mm from the outlet of the mixing chamber should be considered to be the most reliable data. Here, the measured particle temperatures are 2250, 2500, and 2400 K, respectively, at distances of 50, 75, and 120 mm from the chamber outlet. Some increase in the particle temperature at a distance from the chamber outlet testifies to the possibility of prolonged conservation of thermal balance of particles with the plasma and even their heating due to a more prolonged stay in the plasma jet. A subsequent decrease in the particle temperature is associated with their escape from the zone of intense heating.

CONCLUSIONS

1. A heterogeneous plasma jet at the mixing chamber outlet represents a turbulent plasmoid with irregular space-time characteristics. Averaging of the jet structure for times of about 0.1 sec and more leads to the widely adopted representation of a plasma jet in the form of a continuous plasma flow which can be approximated by an inhomogeneous volume of axial symmetry. The degree of inhomogeneity of the plasma jet in cross-section is small as compared to changes in the plasma parameters due to fluctuations, and the distribution of the parameters in this direction can be assumed, with a good approximation, to be uniform.

2. Particle velocities in a plasma jet change from 30 to 80 m/sec, weakly depend on the operation conditions of the installation, and remain unchanged at a distance from the outlet of the mixing chamber of up to 150 mm. For plasma jets there is observed a large deviation of the velocities (30–125 m/sec). The jet velocity markedly decreases as the distance from the chamber outlet increases.

3. In the region of plasma temperatures lower than 6000 K the plasma characteristics, in particular, its emissivity in a continuum, are strongly affected by such easily ionizable admixtures of non-erosion origin as, for instance, sodium and calcium. The calcium concentration is 10% in a plasma jet with phosphate particles and 0.001% with Al_2O_3 particles. Even in the latter case the influence of the admixture is considerable and should be taken into consideration when the particle temperature of the solid phase is determined by methods of optical pyrometry.

4. Introduction of particles of a solid phase into a plasma jet decreases the plasma temperature. In the case of particles of Al_2O_3 powder, chamotte sand, kaolin, and SiO_2 at the outlet of the mixing chamber it is equal to approximately 6000 K, which is lower by 500 K than in the case of a "pure" plasma. The greatest decrease in temperature (up to 4000 K) is observed when phosphates are added to a plasma jet.

5. The temperature of Al_2O_3 measured by methods of optical pyrometry was equal to 2200–2500 K at a distance of more than 50 mm from the outlet of the mixing chamber. In the other cases the continuous plasma radiation was much stronger than the thermal radiation of particles due to easily ionizable admixtures introduced into the plasma jet.

NOTATION

I, current in plasma generator, A; U, voltage drop across plasma generator, V; G_g, flow rate of plasma-forming gas, g/sec; G_p, powder flow rate, g/sec; W, velocity, m/sec; n, concentration, cm^{-3}; T, temperature, K; l, distance, mm; ε, spectral emissivity, $W/(cm^3 \cdot Sr)$; λ, wavelength, nm; X, space coordinate perpendicular to channel axis, mm. Subscripts and superscripts: e, electron, pl, plasma; p, particles; po, powder.

REFERENCES

1. A. L. Mossé and E. M. Ermolaeva, Inzh.-Fiz. Zh., 50, No. 5, 824-828 (1990).
2. E. M. Ermolaeva, E. A. Ershov-Pavlov, A. N. Knak, L. E. Krat'ko, A. L. Mossé, and V. D. Shimanovich, in: Heat and Mass Transfer-95 [in Russian], Minsk (1995), pp. 91-96.
3. V. Lokhte-Khol'tgreven (ed.), Methods of Plasma Investigation [in Russian], Moscow (1971).
4. V. D. Shimanovich, L. E. Krat'ko, N. I. Chubrik, E. A. Ershov-Pavlov, A. L. Mossé, A. N. Knak, and E. M. Ermolaeva, Zh. Prikl. Spektrosk., 63, No. 6, 1054-1061 (1997).
5. A. A. Kurskov, E. A. Ershov-Pavlov, and L. V. Chvyaleva, "Diagnostics of an inhomogeneous low-temperature plasma by the "localization method," Preprint No. 589 of the Institute of Physics of the Academy of Sciences of Belarus, Minsk (1990).
6. I. G. Preobrazhenskii (ed.), Abel Inversion and Its Generalization [in Russian], Novosibirsk (1984).
7. S. V. Dresvin (ed.), Physics and Technology of Plasma [in Russian], Moscow (1972).
8. S. V. Goncharik, A. M. Grigorenko, E. A. Ershov-Pavlov, et al., Pribory Tekhn. Eksper., No. 5, 223 (1985).